Molecular Biology of the Cell
Vol. 13, 3355–3368, September 2002

# Role of LAMP-2 in Lysosome Biogenesis and Autophagy

**Eeva-Liisa Eskelinen,*† Anna Lena Illert,†‡ Yoshitaka Tanaka,‡§ Günter Schwarzmann,¶ Judith Blanz,‡ Kurt von Figura,‡ and Paul Saftig#‖**

*Centre for High Resolution Imaging and Processing, School of Life Sciences, University of Dundee, Dundee DD1 5EH, Scotland, UK; ‡Zentrum Biochemie und Molekulare Zellbiologie, Abt. Biochemie II, Universität Göttingen, 37073 Göttingen, Germany; §Graduate School of Pharmaceutical Sciences, Pharmaceutical Cell Biology, Kyushu University, Fukuoka, Japan; ¶Kekule Institut für Organische Chemie und Biochemie der Universität, D-53121 Bonn, Germany; and #Biochemisches Institut, Universität Kiel, D-24098 Kiel, Germany

Submitted February 28, 2002; Revised June 12, 2002; Accepted June 28, 2002
Monitoring Editor: Jennifer Lippincott-Schwartz

In LAMP-2–deficient mice autophagic vacuoles accumulate in many tissues, including liver, pancreas, muscle, and heart. Here we extend the phenotype analysis using cultured hepatocytes. In LAMP-2–deficient hepatocytes the half-life of both early and late autophagic vacuoles was prolonged as evaluated by quantitative electron microscopy. However, an endocytic tracer reached the autophagic vacuoles, indicating delivery of endo/lysosomal constituents to autophagic vacuoles. Enzyme activity measurements showed that the trafficking of some lysosomal enzymes to lysosomes was impaired. Immunoprecipitation of metabolically labeled cathepsin D indicated reduced intracellular retention and processing in the knockout cells. The steady-state level of 300-kDa mannose 6-phosphate receptor was slightly lower in LAMP-2–deficient hepatocytes, whereas that of 46-kDa mannose 6-phosphate receptor was decreased to 30% of controls due to a shorter half-life. Less receptor was found in the Golgi region and in vesicles and tubules surrounding multivesicular endosomes, suggesting impaired recycling from endosomes to the Golgi. More receptor was found in autophagic vacuoles, which may explain its shorter half-life. Our data indicate that in hepatocytes LAMP-2 deficiency either directly or indirectly leads to impaired recycling of 46-kDa mannose 6-phosphate receptors and partial mistargeting of a subset of lysosomal enzymes. Autophagic vacuoles may accumulate due to impaired capacity for lysosomal degradation.

## INTRODUCTION

Lysosomes are acidic membrane-bound organelles containing hydrolytic enzymes for degradation of proteins, lipids, nucleic acids, and polysaccharides. Lysosomal enzymes are synthesized in the endoplasmic reticulum and sorted in the trans-Golgi network (TGN) by mannose 6-phosphate receptors (MPRs). MPRs bind the mannose 6-phosphate tag of lysosomal enzymes in the trans-Golgi network (TGN), and the receptor-ligand complexes are transported to endosomes in clathrin-coated vesicles. In endosomes ligands dissociate from the MPRs due to the acidic pH, and receptors may then recycle back to TGN. A small proportion of newly synthesized lysosomal enzymes is secreted to the extracellular medium (Jadot *et al.*, 1997). Mammalian cells contain two different MPRs, the cation-independent or 300-kDa MPR, and the cation-dependent or 46-kDa MPR. Both receptors are needed for efficient intracellular retention of lysosomal enzymes (Kasper *et al.*, 1996). In addition MPRs also recycle between early endosomes and the plasma membrane. However, only MPR300 is able to mediate endocytosis of exogenous mannose 6-phosphate containing ligands (Hille-Rehfeld, 1995).

The limiting membrane of the lysosomal compartment has multiple functions. It is responsible for acidification of the

Article published online ahead of print. Mol. Biol. Cell 10.1091/mbc.E02–02–0114. Article and publication date are at www.molbiolcell.org/cgi/doi/10.1091/mbc.E02–02–0114.

‖ Corresponding author. E-mail address: psaftig@biochem.uni-kiel.de.

† Both authors contributed equally to this work.

Abbreviations used: Avi, early autophagic vacuole; Avd, late autophagic vacuole; BSA, bovine serum albumin; ER, endoplasmic reticulum; LAMP, lysosomal associated membrane protein; LBPA, lysobisphosphatidic acid; 3MA, 3-methyladenine; MPR, mannose 6-phosphate receptor; TGN, trans-Golgi network.

© 2002 by The American Society for Cell Biology

interior, sequestration of the active lysosomal enzymes (Kornfeld and Mellman, 1989), and transport of degradation products from the lysosomal lumen to the cytoplasm (Lloyd and Forster, 1986; Fukuda, 1991; Peters and von Figura, 1994). The lysosomal membranes contain several highly N-glycosylated proteins including LAMP-1 and LAMP-2. These two glycoproteins are structurally similar and evolutionary related (Granger *et al.*, 1990). Like LAMP-1, LAMP-2 is composed of a large luminal portion, which is separated by a proline-rich hinge region in two disulphide containing domains, a single transmembrane-spanning segment, and a short cytoplasmic tail of 11 amino acids (Lewis *et al.*, 1985; Fambrough *et al.*, 1988). The latter contains a Gly-Tyr motif critical for transport to lysosomes (Guarnieri *et al.*, 1993; Höning and Hunziker, 1995). LAMP-2 is one of the major carriers for poly-*N*-acetyllactosamines in cells (Fukuda, 1991).

Although the ubiquitously expressed LAMP-2 is localized primarily in the late endosomes and lysosomes (Lippincott-Schwartz and Fambrough, 1987), under certain circumstances, e.g., after platelet activation, during granulocytic differentiation and activation, in malignant carcinoma cells, and in cytotoxic T lymphocytes, it is also found at the cell surface (Febbraio and Silverstein, 1990; Lee *et al.*, 1990). LAMP-2 has also been described as a receptor for the selective import and degradation of cytosolic proteins in the lysosome, or chaperone-mediated autophagy (Cuervo and Dice, 1996, 1998).

Autophagy is a central mechanism in cellular metabolism that cells use to degrade parts of their cytoplasm and organelles using lysosomal enzymes. The autophagic-lysosomal pathway is known to play an important role in the cellular protein economy (Mortimore *et al.*, 1989; Seglen and Bohley, 1992). In hepatocytes exposed to nutrient starvation it can account for as much as three quarters of the overall protein degradation (Mortimore *et al.*, 1989; Seglen and Bohley, 1992). The first step in autophagy is segregation of cytoplasm by a membrane cisterna, which forms a double or multiple membrane-bound vacuole called the autophagosome. Autophagosomes acquire lysosomal membrane proteins, vacuolar proton pumps, and acid hydrolases, presumably by fusing with endosomes/lysosomes. Finally, the contents are degraded by lysosomal enzymes (Arstila and Trump, 1968; Dunn, 1994; Klionsky and Emr, 2000). The autophagic pathway is subject to complex regulation, it is activated in mammalian cells by amino acid deprivation (Mitchener *et al.*, 1976; Seglen, 1987; Talloczy *et al.*, 2002).

LAMP-2 deficiency leads to premature postnatal death of about half of all LAMP-2–deficient mice (Tanaka *et al.*, 2000). In several LAMP-2–deficient tissues, including muscle, heart, pancreas, and liver, an accumulation of autophagic vacuoles was observed. We also observed a reduced contractile function of the heart muscle. Thus, LAMP-2–deficient mice represent a valuable animal model for autophagic vacuolar myopathy, or Danon disease, a human disease associated with a mutated LAMP-2 gene (Nishino *et al.*, 2000). Here we extend the phenotype analysis of these mice using cultured hepatocytes.

## MATERIALS AND METHODS

### *Primary Antibodies*

The following antibodies were used in this study: Rabbit antiserum against mouse cathepsin D (Pohlmann *et al.*, 1995), rabbit antiserum against rat liver cathepsin D purified from lysosomal contents by affinity chromatography on pepstatin A-sepharose as described (Yamamoto *et al.*, 1979), affinity-purified rabbit antibody against the cytoplasmic tail of MPR46 (MSC1; Klumperman *et al.*, 1993), rabbit antiserum against human MPR46 (II-4; Wenk *et al.*, 1991), rabbit antiserum against rat MPR300 (I-5; Claussen *et al.*, 1995), mouse mAb against γ-adaptin (Transduction Laboratories, Lexington, KY), and rat monoclonal antibodies against LAMP-2 (ABL93) and LAMP-1 (1D4B; Developmental Studies Hybridoma Bank, Iowa City, Iowa).

### *Preparation of Primary Mouse Hepatocytes*

Mouse hepatocytes were prepared from 3- to 6-month-old mice according to a described procedure (Meredith, 1988). Hepatocytes were enriched using a Percoll gradient (58% wt/vol) and plated on collagen-coated or -uncoated plastic culture dishes. Unless stated otherwise, the cells were cultured overnight in RPMI-1640 containing 10% fetal calf serum (FCS) and penicillin/streptomycin (Life Technologies, Rockville, MD) before the experiments.

### *Endocytic Uptake*

Six-nanometer gold particles were prepared (Slot and Geuze, 1985) and coated with bovine serum albumin (BSA). BSA-gold was dialyzed against RPMI-1640 medium and diluted to serum-free RPMI containing 0.2% BSA. After uptake the cells were rinsed and fixed for electron microscopy.

### *Immunofluorescence*

Hepatocytes were grown on glass coverslips. The cells were fixed with cold methanol or 4% paraformaldehyde in 0.1 M HEPES, pH 7.4, and permeabilized with 0.5% saponin or 0.1% Triton X-100. The cells were immunostained using antibodies against MPR46. The primary antibodies were detected with goat anti-rabbit IgG conjugated with Texas red or fluorescein (Dianova GmbH, Hamburg, Germany). After embedding in Mowiol (Calbiochem-Novabiochem GmbH, Bad Soden, Germany) containing DABCO, fluorescence was examined using a confocal laser-scanning microscope (LSM 2; Zeiss, Oberkochen, Germany).

### *Western Blotting*

Expression of cathepsin-D, MPR46, and MPR300 was analyzed in hepatocyte homogenates (cathepsin D) and membrane fractions (receptors). Hepatocytes were homogenized in Tris-buffered saline (wt/vol; 1:9) at 4°C using an Ultra-Turrax, and the homogenate was analyzed for protein content. To obtain membrane fractions cell pellets were resuspended in TBS including proteinase inhibitors, subjected to sonication (3 times, 200 s), and pelleted at high speed (100,000 × *g*). The resulting pellet was resuspended in TBS/proteinase inhibitors/1% Triton X-100 and subjected to sonication (3 times, 20 s). One hundred micrograms of protein was subjected to SDS-PAGE (5% polyacrylamide in case of MPR300; 10% in case of MPR46 and cathepsin D) under reducing conditions. Proteins were transferred to a polyvinylidene difluoride membrane (Schleicher & Schüll, Dassel, Germany), which was subsequently blocked with 10 mM PBS, pH 7.4, 0.05% Triton X-100, 5% milk powder (blocking buffer) for 1 h at 37°C. The blot was incubated overnight at 4°C with rabbit anti-mouse cathepsin-D, anti-MPR46 MSC1, or anti-MPR300 serum. Membranes were washed six times for 5 min in 10 mM PBS, pH 7.4, 0.1% Tween 20. Subsequently, incubation with horseradish peroxidase–coupled anti-rabbit antibody was performed for 1 h at room temperature followed by washing six times for 5 min in 10 mM PBS, pH 7.4, 0.1% Tween 20. Blots were finally analyzed using the ECL Detection System (Amersham Pharmacia Biotech, Piscataway, NJ). Quantification was performed by densitometry (Scan Jet 4c/T; Hewlett-Packard, Palo Alto, CA; WinCam 2.2).

### *Metabolic Labeling and Immunoprecipitation*

Hepatocytes were incubated in methionine-free medium for 1 h and then labeled with $^{35}$S-methionine/cysteine (Amersham Life Science, Inc., Rockville, MD) in the same medium containing 5% dialyzed FCS. During the chase, the medium was supplemented with 0.25 mg/ml L-methionine/L-cysteine. Immunoprecipitation from cells and media was carried out as described previously (Waheed *et al.*, 1988) with rabbit antibodies against cathepsin-D, MPR46 (II-4), or MPR300. Densitometric quantification of the bands was done with a phosphoimager (Fuji, Stamford, CT) and the program MacBas.

### *Incubation of Cells with Radioactive Glucosylthioceramide and thioGM3*

An aliquot of a stock solution of the desired glucosylthioceramide and thioGM3 in methanol was dried under a stream of nitrogen. The dried lipid was dissolved by first adding 20 $\mu$l of ethanol and then 0.75 ml of RPMI containing 5 mg of defatted BSA under vigorous stirring. The resulting solution was diluted with 6.85 ml of RPMI to yield a 10 $\mu$M lipid-BSA complex.

Hepatocytes seeded on 6-cm dishes were washed in RPMI and incubated with the [$^{14}$C]$C_8$-Glc-S-Cer/BSA complex or the [$^{14}$C]thioGM3/BSA complex in RPMI for 3 h at 37°C, washed with PBS, and further incubated for 24 h at 37°C in RPMI containing 5% heat-inactivated FCS. The incubation media were saved, and the cells were washed with PBS, harvested with a rubber policeman, and centrifuged at 2000 × *g* for 10 min. For protein determination, the pellet was suspended in 0.4 ml of $H_2O$, and 5-$\mu$l aliquots were assayed. The lipids were extracted with 4 ml of chloroform/methanol (1:1, by volume) for 3 h at 38°C. The lipid extracts and the media were desalted according to Williams and McCluer (1980). Total radioactive lipids of both cells and media were determined by liquid scintillation counting of aliquots. The lipid extracts of cells and media were analyzed by TLC using chloroform/methanol/15 mM calcium chloride (60:35:8, by volume) as the developing solvent. In addition, TLC plates were exposed to x-ray film (Kodak X-Omat XAR-5; Eastman Kodak, Rochester, NY).

### *Northern Blotting*

Total RNA of cultured hepatocytes was prepared using the Qiagen Rneasy system (Hilden, Germany). Ten micrograms of total RNA were separated in a formaldehyde agarose gel and processed as described (Isbrandt *et al.*, 1994). Filters were hybridized with a MPR46 and MPR300 cDNA probe (Köster *et al.*, 1991) and a $\beta$-actin probe (CLONTECH, Palo Alto, CA). Hybridization and washing of the filters were performed as described (Lehmann *et al.*, 1992).

### *Electron Microscopy and Autophagosome Quantification*

Isolated hepatocytes were fixed in 2% glutaraldehyde in 0.2 M HEPES, pH 7.4, at room temperature for 2 h. The cells were scraped off the culture dish, pelleted, and postfixed in 1% osmium tetroxide in 0.1 M phosphate buffer for 1 h. The cells were dehydrated in ethanol and embedded in Epon. For estimation of volume fractions by stereology (Howard and Reed, 1998), 20–25 micrographs, primary magnification ×10,000, were taken with systematic random sampling from each sample. The cytoplasmic volume fraction of autophagic vacuoles was estimated by point counting. Autophagic vacuoles were classified as early, containing morphologically intact cytoplasm, and late, containing partially degraded but identifiable cytoplasmic material (Tanaka *et al.*, 2000). Statistical significance was estimated using Student's *t* test.

### *Immunogold Electron Microscopy and Quantitation*

Cultured hepatocytes were fixed in 4% paraformaldehyde in 0.2 M HEPES, pH 7.4, at room temperature for 2 h and then stored in 2% paraformaldehyde for up to 4 d. Some samples were fixed by adding 0.1% glutaraldehyde to the initial fixative. The cells were then embedded in gelatin and processed for cryosectioning as described (Andrejewski *et al.*, 1999). Cryosections were picked up with 2.3 M sucrose or a mixture of sucrose and 2% methyl cellulose. The sections were labeled with rabbit antibodies against MPR46 (MSC1), mouse anti–$\gamma$-adaptin, or rat anti–LAMP-1 or –LAMP-2. The primary antibodies were detected with goat anti-rabbit-IgG, goat anti-rat-IgG, or goat anti-mouse IgG coupled to 5 or 10 nm gold (British BioCell, Cardiff, UK). Double labelings were done by mixing two primary antibodies, from different species, and the corresponding secondary antibodies, conjugated to different sized gold particles. The smaller gold size was used for the less abundant antigen. Density of LAMP-2 labeling on the limiting membranes of autophagic vacuoles was estimated as described (Tanaka *et al.*, 2000). To quantitate the distribution of MPR46 labeling, the sections were systematically screened under the electron microscope, and each time a gold particle was seen, it was recorded into a certain cellular compartment, as explained in Table 2, or into an unrecognizable compartment. To estimate MPR46 labeling in endosome associated tubular and vesicular structures (Klumperman *et al.*, 1993), LAMP-1–positive multivesicular endosomes of 200–800-nm diameter (Figure 8, B–D) were systematically scored. Gold particles situated inside and outside, within a distance of 300–400 nm of the endosomes, were counted. At least 40 endosomal profiles, from two independent samples, were counted, and the results were expressed as a ratio of gold inside/gold outside.

### *Enzyme Activities*

Hepatocytes were isolated and cultured overnight. After washing with PBS the cells were incubated in RPMI medium containing 5% heat-inactivated FCS. After 6, 12, and 24 h, samples of the medium were removed and cells were washed, scraped, and homogenized in TBS/1% Triton X-100. Lysosomal enzyme activities were detected using fluorometric and colorometric assays as described (Köster *et al.*, 1993). To avoid a possible effect of the medium change leading to nonspecific increase of lysosomal enzyme activities, the enzyme activity in the medium after 6-h culture was withdrawn from the specific activities measured in the medium after 12 and 24 h. In each experiment the enzyme activities were measured from two parallel culture dishes. Statistical significance was evaluated using Student's *t* test.

## RESULTS

We observed accumulation of both early autophagic vacuoles (Avi), containing morphologically intact cytoplasm, and late autophagic vacuoles (Avd), containing partially degraded cytoplasmic material, in liver and cultured hepatocytes of LAMP-2–deficient mice (Tanaka *et al.*, 2000). We performed immunogold labeling of control hepatocytes to examine the presence of LAMP-2 in autophagic vacuoles and detected labeling in both Avi and Avd (for Avi see Figure 1). Quantitation of LAMP-2 labeling on the limiting membrane showed that the labeling in Avd was five times higher than that in Avi. This enrichment of LAMP-2 in Avd is similar to that observed for LAMP-1 (Tanaka *et al.*, 2000).

### *Half-life of Autophagic Vacuoles*

Long-lived protein degradation is decreased in LAMP-2–deficient hepatocytes (Tanaka *et al.*, 2000), suggesting that autophagic vacuoles accumulate because of impaired degradation of autophagocytosed material. To clarify this, we determined the half-life of autophagic vacuoles using quantitative electron microscopy. Isolated hepatocytes were in-

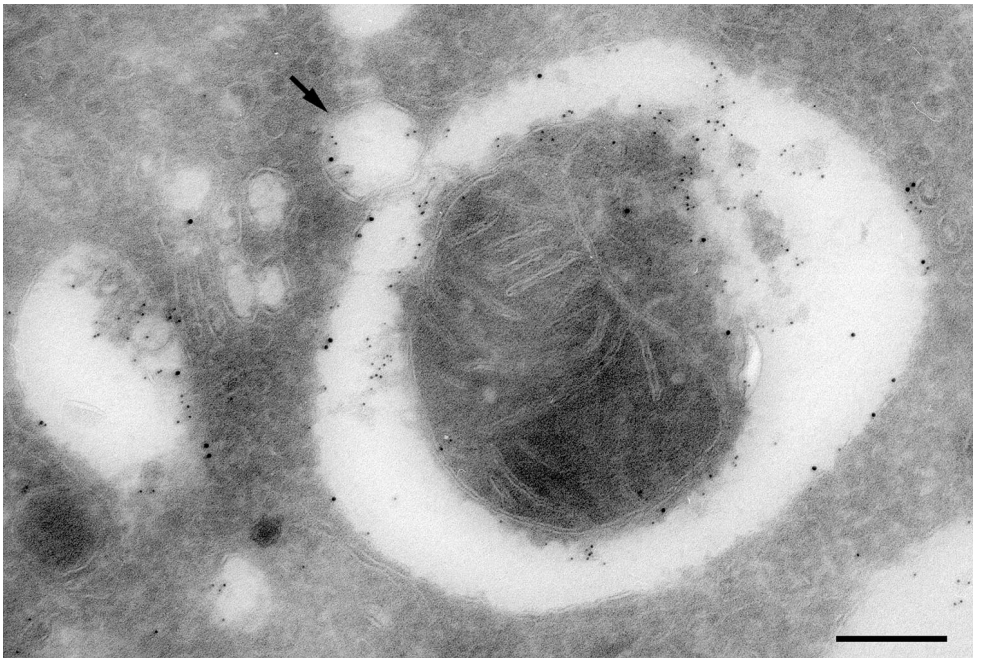

**Figure 1.** LAMP-2 localizes to autophagic vacuoles in control hepatocytes. Isolated hepatocytes were cultured overnight, fixed, and processed for cryosectioning. Thin frozen sections were immunogold labeled for LAMP-2 (10 nm gold) and cathepsin-D (5 nm gold). LAMP-2 localizes to the limiting membrane of the autophagic vacuole, which can be identified by its cytoplasmic contents (a mitochondrion) as an Avi. Cathepsin-D is found in the space between the limiting membrane and the contents of the vacuole. The arrow indicates a vesicle, containing both LAMP-2 and cathepsin-D, that is likely to be in the process of fusion with the autophagic vacuole. Bar, 200 nm.

cubated in starvation medium (free of serum and amino acids) for 5 h to induce autophagy. Subsequently the fate of the autophagic vacuoles was followed by shifting the cells to FCS containing medium, supplemented with 10 mM 3-methyladenine (3MA) to prevent formation of new autophagosomes (Seglen and Gordon, 1982, 1984). Samples for electron microscopy were taken before the starvation, after 5-h starvation, and 1- and 3-h chase in full medium with 3MA, as indicated in Figure 2. The volume fractions of Avi, Avd, and endosomes/lysosomes were estimated using stereology. The latter compartment included all endo/lysosomal vesicles lacking morphologically identifiable cytoplasmic material, i.e., early and late endosomes and lysosomes. In control cells (Figure 2, A and B) the volume fraction of Avi and Avd increased ~3.8-fold ($p = 0.0012$) and 1.7-fold ($p = 0.078$), respectively, during 5-h starvation. After 1-h chase in full medium with 3MA, almost all Avi had disappeared from the control cells ($p = 0.000015$ compared with the 5-h starvation). This suggests that Avi matured into Avd and these in turn degraded their contents. During the 3-h chase the size of Avd decreased in control cells ($p = 0.047$ compared with the 5-h starvation), suggesting further degradation of the cytoplasmic material.

Consistent with our previous findings (Tanaka *et al.*, 2000), the volume fractions of both Avi and Avd were much higher in LAMP-2–deficient hepatocytes. Also the volume fraction of endo/lysosomes was twice as high as in the control cells (Figure 2, A–C). Starvation did not increase the volume fraction of total Avi/Avd/endo/lysosomal pool in LAMP-2–deficient cells, suggesting that autophagy cannot be further stimulated by starvation. However, we observed a small increase in Avd volume fraction ($p = 0.041$) on the expense of endo/lysosomes ($p = 0.051$). During the 1-h chase in full medium and 3MA, less than half of the Avi volume fraction was consumed ($p = 0.016$), indicating retarded conversion of Avi into Avd. Approximately corresponding increase was observed in the volume fraction of endo/lysosomes ($p = 0.0029$), which suggests initial maturation of some Avd into lysosomes. During the 3-h chase no further decrease of Avi volume fraction was observed, whereas the volume of Avd tended to increase ($p = 0.08311$ compared with the 5-h starvation). This increase in Avd may point to fusion with plasma membrane derived endosomes, which would increase the volume fraction similar to maturation of Avi into Avd. The results indicate that in LAMP-2–deficient hepatocytes the consumption of Avd is severely retarded and that the half-lives of both Avi and especially Avd are prolonged.

### *Fusion of Endosomes with Autophagic Vacuoles*

In LAMP-2–deficient hepatocytes the pH in Avi and Avd is only slightly higher than in control cells and the limiting membranes of Avd contain substantial amounts of LAMP-1 (Tanaka *et al.*, 2000). This suggests that transport of membrane proteins such as the vacuolar proton pump and LAMP-1 to Avi and/or Avd does take place. To directly demonstrate the convergence of endocytic and autophagic pathways we used 6-nm gold particles coated with BSA (BSA-gold) as a fluid phase endocytic tracer. To check that the knockout hepatocytes are able to perform fluid-phase endocytosis at rates comparable to that of the control cells, the cells were fed with horseradish peroxidase for 10–30 min and washed, and the peroxidase activity was assayed from cell homogenates. The results revealed that the rate of fluid-phase uptake is comparable in LAMP-2–deficient and control hepatocytes. BSA-gold was then fed to cells for 1 h, and the cells were chased for 2 h. Electron microscopy was used to score the distribution of gold particles in endo/lysosomes and autophagic vacuoles. Typical fusion profiles of Avd and multivesicular endosomes in LAMP-2–deficient cells are presented in Figure 3, A and B. In control cells, ~20% of gold

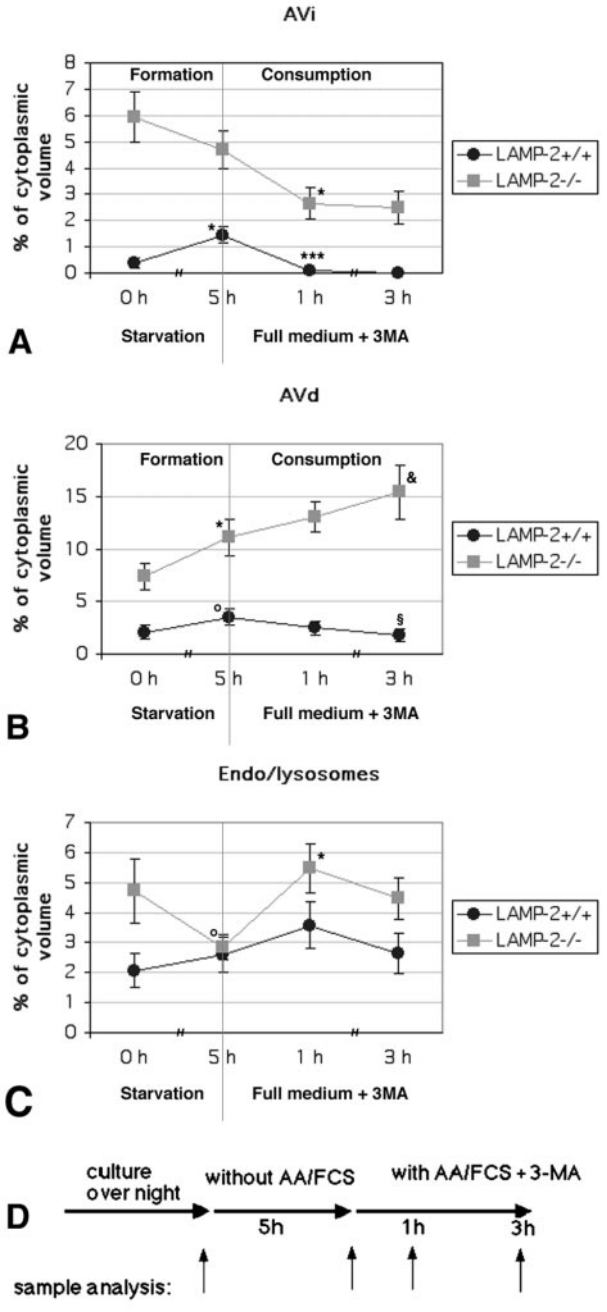


**Figure 2.** Half-life of autophagic vacuoles in control and LAMP-2–deficient hepatocytes. The cells were cultured overnight and then starved for serum and amino acids for 5 h to induce autophagy. Subsequently the cells were shifted to serum and amino acid–containing culture medium (full medium), including 10 mM 3MA. Samples for quantitative electron microscopy were taken as indicated in D. Cytoplasmic volume fractions of early (Avi, A) and late (Avd, B) autophagic vacuoles and endo/lysosomes (C) were estimated by point counting. The results are the mean ± SEM from two independent experiments; a minimum of 40 micrographs were quantitated for each time point. Statistical significance compared with the previous time point on the same graph: *, $0.00122 < p < 0.042$; ***, $p = 0.000015$; °, $0.05 < p < 0.079$. Statistical significance compared with the 5-h time point on the same graph: &, $p = 0.08311$; §, $p = 0.04716$.

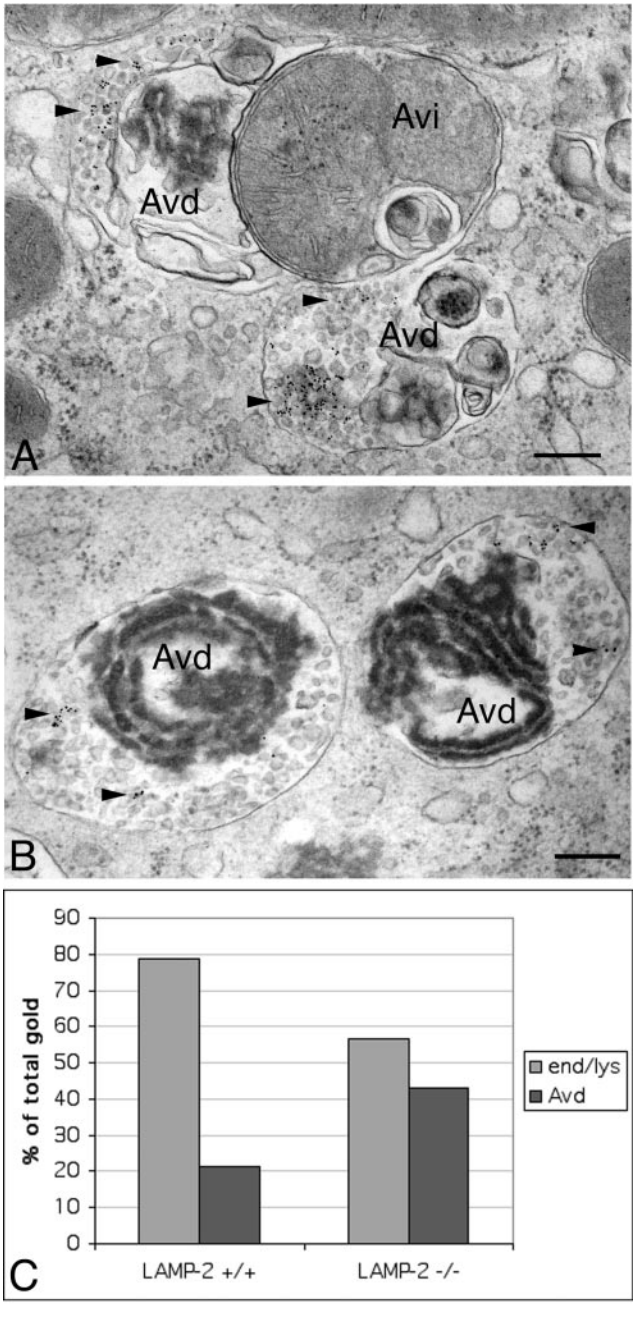


**Figure 3.** Endocytosed BSA-gold is transported to autophagic vacuoles in LAMP-2–deficient cells. Cells were fed with BSA-gold for 1 h, chased in full culture medium for 2 h, and subsequently fixed and processed for electron microscopy. (A and B) Typical fusion profiles of multivesicular endosomes and autophagic vacuoles in LAMP-2–deficient cells. The arrowheads indicate the BSA-gold, which is associated with small vesicles. Autophagic vacuoles were identified by their cytoplasmic contents: electron dense, partially degraded ribosomes or rough ER (Avd) or a mitochondrion (Avi). No BSA-gold was found in early autophagic vacuoles. Bars, 200 nm. (C) Distribution of the endocytic tracer between autophagic vacuoles and endo/lysosomes (end/lys) was estimated by systematically screening the thin sections. A total of 1469 and 2186 gold particles were screened from control and LAMP-2 −/− cells, respectively.

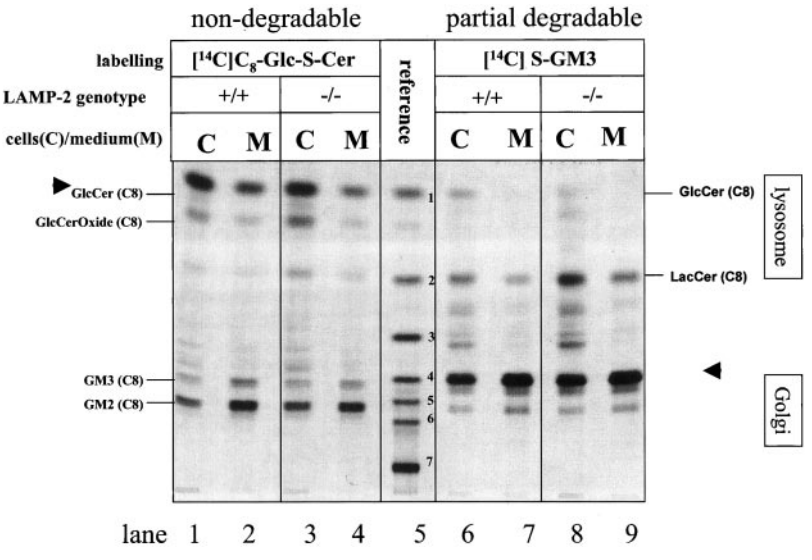


**Figure 4.** Postendocytotic glycosylation of [$^{14}$C]$C_8$-Glc-S-Cer and of catabolites of thioganglioside [$^{14}$C]$C_8$-SGM3 in control and LAMP-2–deficient hepatocytes. Mouse hepatocytes were incubated with [$^{14}$C]$C_8$-Glc-S-Cer (lanes 1–4) and [$^{14}$C]$C_8$-S-GM3 (lanes 6–9) as described in MATERIALS AND METHODS. After 3-h labeling the cells were chased for another 24 h. The chase media were saved, and the cells were harvested. The desalted lipids of cells and chase media were separated by TLC using chloroform/methanol/15 mM calcium chloride (60:35:8, by volume) as a developing system. The radioactive lipids were visualized by exposure to x-ray–sensitive film. Lane 5, reference lipids from top to bottom: 1, [$^{14}$C]$C_8$-Glc-S-Cer; 2, [$^{14}$C]$C_8$-Lac-S-Cer; 3, [$^{14}$C]$C_8$-$GbOse_3$Cer; 4, [$^{14}$C]$C_8$-S-GM3; 5, [$^{14}$C]$C_8$-S-GM2; 6, [$^{14}$C]$C_8$-S-GM1; 7, [$^{14}$C]$C_6$-GD1a with their relative mobilities denoted by standard abbreviations for GSL as explained in Schwarzmann *et al.* (1995). In addition the mobilities of *N*-glycolyl neuraminic acid containing thiogangliosides GM3 and GM2 denoted as NeuGc-GM3 and NeuGc-GM2 are indicated, respectively. Their endogenous counterparts are the predominant gangliosides in murine hepatocytes and are formed by sialylation of lactosylceramide with CMP-NeuGc as the activated sugar. GM3 cannot be transformed directly into NeuGc-GM3 or NeuGc-GM2. Arrowheads indicate the labeled glycosphingolipids that were fed to the hepatocytes.

particles were found in Avd, compared with >40% in LAMP-2–deficient hepatocytes (Figure 3C). The larger fraction of gold in Avd in LAMP-2–deficient cells may be due to the prolonged half-life of these organelles, resulting in trapping of the tracer within Avd. The result indicates that multivesicular endosomes are able to fuse with autophagic vacuoles in LAMP-2–deficient hepatocytes.

### *Trafficking of Lipids between the Plasma Membrane, Lysosomes, and the Golgi*

We studied the uptake of the nondegradable glycosphingolipid glucosylthioceramide ([$^{14}$C]$C_8$-Glc-S-Cer). A fraction of the internalized glucosylthioceramide is transported to the Golgi as indicated by its elongation to GM2 and GM3 by Golgi resident glycosyltransferases (Schwarzmann and Sandhoff, 1990; Schwarzmann *et al.*, 1995; Schwarzmann, 2001). The glucosylthioceramide was taken up by control and LAMP-2–deficient hepatocytes. In both genotypes Golgi-specific glycosylation products (e.g., GM2 and GM3) were detected to a comparable level in cells and media (Figure 4, lanes 1–4). The appearance of glycosylation products in culture media containing FCS is due to transport of the glycosylation products from the Golgi apparatus to the plasma membrane and to the extraction of the semitruncated glycolipids by protein components of the FCS.

Having shown that hepatocytes allow efficient uptake and trafficking of labeled sphingolipids, we studied the metabolism of the partially degradable thioganglioside ([$^{14}$C]S-GM3). This compound allows to follow the trafficking of the internalized thioganglioside to endosomes/lysosomes, where it is degraded to glycosylthioceramide, and the trafficking of glucosylthioceramide to the Golgi where it is elongated to GM2 and GM3. GM2 and GM1 originating from elongation of the added GM3 contain neuraminic acid. In contrast, the GM3, GM2, and GM4 originating from glucosylthioceramide generated from the added GM3 in the lysosomes contain the hepatocyte derived *N*-glycolyl-neuraminic acid and are thereby distinguishable (Schwartzmann, 2001). The uptake, accumulation, and degradation in lysosomes and the subsequent transport of the labeled lipids to the Golgi apparatus and elongation to *N*-glycolyl neuraminic acid containing thiogangliosides GM3 and GM2 were similar in LAMP-2–deficient and control hepatocytes (Figure 4, lanes 6–9). This indicates that transport of lipids from the plasma membrane to lysosomes and from there to the Golgi apparatus is not affected by LAMP-2 deficiency.

### *Activities and Trafficking of Lysosomal Enzymes*

The prolonged half-life of autophagic vacuoles could result from impaired degradation of their content. Impaired acidification as a cause for compromised lysosomal degradation has already been excluded (Tanaka *et al.*, 2000). We therefore determined the activities of lysosomal enzymes in isolated hepatocytes and liver homogenates as well as the trafficking and maturation of newly synthesized cathepsin D, a major lysosomal proteinase. The activities of three representative lysosomal hydrolases were differentially affected in LAMP-2–deficient hepatocytes. Intracellular β-mannosidase activity of LAMP-2–deficient hepatocytes was decreased to ~14% of control ($p = 0.022$), β-glucuronidase was unchanged, and β-hexosaminidase seemed to be increased about twofold, although this increase was not statistically significant (Table 1). Interestingly, the activity of β-mannosidase was only moderately affected in liver homogenates of LAMP-2–deficient mice ($0.43 \pm 0.03$ vs. $0.59 \pm 0.08$ U/g in control liver). This indicates that the β-mannosidase activity in nonparenchymal liver cells is normal. The fraction of enzyme activity recovered in the secretion was elevated 2.55–4.7-fold for β-mannosidase ($p = 0.022$) and β-glucuronidase ($p = 0.017$) and not affected for β-hexosaminidase (Table 1). This indicates mistargeting of a subset of lysosomal enzymes into the culture medium.

**Table 1.** Lysosomal enzyme activities in control and LAMP-2–deficient hepatocytes

| | Control | | LAMP-2 −/− | |
|---|---|---|---|---|
| | Cells (mU/mg) | Medium (% of total) | Cells (mU/mg) | Medium (% of total) |
| β-Mannosidase | 1.33 ± 0.33 (3) | 5.7 ± 0.79 | 0.19 ± 0.07 (4) p = 0.022* | 14.53 ± 0.02 p = 0.022* |
| β-Hexosaminidase | 8.28 ± 3.5 (2) | 17.09 ± 1.0 | 16.54 ± 3.5 (2) p = 0.12 | 15.64 ± 0.86 p = 0.19 |
| β-Glucuronidase | 3.13 ± 0.55 (2) | 1.83 ± 0.63 | 3.45 ± 0.26 (2) p = 0.67 | 8.61 ± 0.24 p = 0.017* |

Values are means ± SEM; number of independent cultures used for each value is given in parentheses.
* p values indicating statistical significance of the difference between the control and LAMP-2 −/− cells.

Cathepsin-D was quantified in hepatocytes by Western blotting. The total amount of cathepsin-D was decreased ~2.5-fold in LAMP-2–deficient hepatocytes. In particular the amount of the catalytically active forms of cathepsin-D, the 46-kDa processing intermediate, and the mature 30- and 14-kDa polypeptides were decreased in LAMP-2–deficient hepatocytes, whereas that of the 52-kDa precursor form was increased (Figure 5A).

The 3- to 5-fold higher fraction of β-mannosidase and β-glucuronidase in the secretions (Table 1) and the decrease of proteolytically processed cathepsin-D forms in the hepatocytes points to a missorting of newly synthesized lysosomal enzymes into the secretions. To follow the fate of newly synthesized cathepsin-D, hepatocytes were metabolically labeled, and cathepsin-D was immunoprecipitated from cells and media (Figure 5B). We observed in LAMP-2–deficient cells an increased secretion of cathepsin-D. After 6-h chase, 47% of cathepsin-D was recovered in the secretions and 21% had been proteolytically processed to the 46-kDa intermediate. In control hepatocytes 14% had been secreted, and 68% were proteolytically processed to the catalytically active intermediate.

Taken together these results show that missorting contributes to the lower levels of cathepsin-D in LAMP-2–deficient hepatocytes and possibly also to the intracellular deficiency of β-mannosidase as well as to the increased proportion of β-glucuronidase in the culture medium.

### *Expression of MPR300*

Missorting of cathepsin-D and two other lysosomal enzymes into secretion suggested that LAMP-2–deficient hepatocytes might have a defect in the function of MPRs. We first investigated the expression of MPR300. Western blotting showed

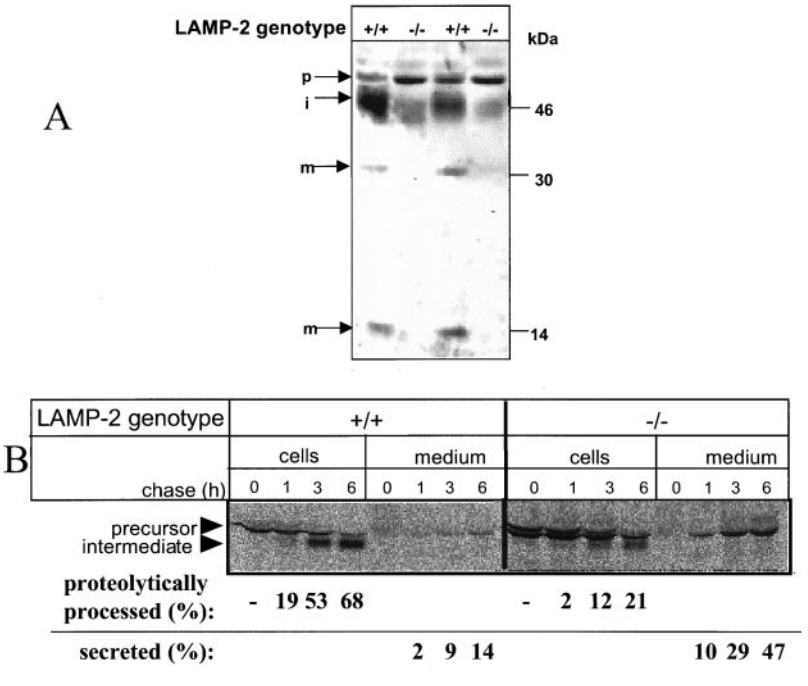


**Figure 5.** Intracellular sorting of cathepsin D is impaired in LAMP-2–deficient cells. (A) Western blotting of cathepsin-D from control (+/+) and LAMP-2 −/− cells. p, precursor; i, intermediate; and m, mature form of the enzyme. Equal amounts of protein were loaded in each lane. (B) Immunoprecipitation of cathepsin-D. The cells were labeled with [$^{35}$S]methionine for 1 h and then chased as indicated. Cathepsin-D was immunoprecipitated from the cells and culture medium. The bands were quantitated by densitometry.

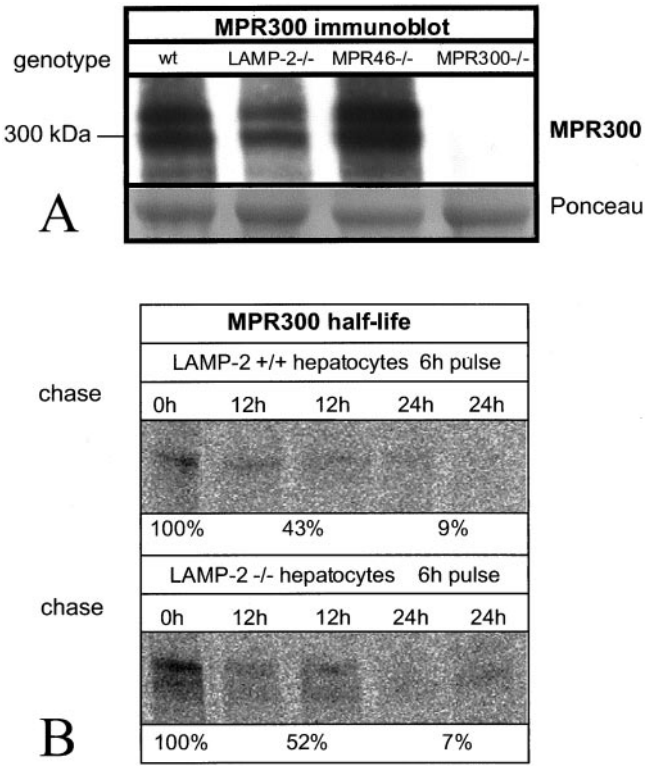


**Figure 6.** Steady state levels of MPR300. (A) Western blotting and of MPR300 in control (wt), LAMP-2 −/−, MPR46−/−, and MPR300 −/− cells. Ponceau-stained bands are shown as a loading control. (B) Immunoprecipitation of MPR300 after 6-h pulse with radioactive methionine followed by chase for 0, 12, and 24 h. Densitometric quantitation of the bands is also shown.

comparable protein levels in control and LAMP-2–deficient hepatocytes (Figure 6A). Densitometric quantitation from 17 independent cultures revealed that LAMP-2–deficient cells had 78.3 ± 22.6% (mean ± SD) of the protein level found in control hepatocytes. Metabolically labeled MPR300 had comparable half-lives in control and LAMP-2–deficient hepatocytes (Figure 6B).

### *Half-life and Localization of MPR46*

We next performed Western blotting of MPR46 (Figure 7A). Densitometric quantitation of bands from 10 independent cultures revealed that the steady state level of MPR46 was reduced to 27.5 ± 8.9% of controls in LAMP-2–deficient hepatocytes. However, Northern blotting showed that the level of MPR46 mRNA was comparable to the control (Figure 7B). Stability of metabolically labeled MPR46 showed MPR46 to have a shortened half-life in LAMP-2–deficient hepatocytes: 41–42% of newly synthesized receptor was recovered in LAMP-2–deficient cells after 12-h chase (Figure 7C), compared with 96% in control cells. Addition of lysosomal protease inhibitors, leupeptin and pepstatin, to the chase medium rescued the half-life in knockout cells to control level (Figure 7C), suggesting that degradation by lysosomal proteinases contributes to the shorter half-life.

The shortened half-life of MPR46 prompted us to study its intracellular localization. Immunofluorescence showed that in control cells MPR46 was localized to the perinuclear region as vesicular-reticular labeling (Figure 7D), consistent with earlier results showing that MPR46 is located in the TGN, endosomes, and small cytoplasmic vesicles (Klumperman *et al.*, 1993). In the LAMP-2–deficient hepatocytes MPR46 labeling was observed in only 42% of cells, whereas 95% of control hepatocytes showed labeling. Thus, there is an apparent inconsistency between the Western blot (27.5% the protein level of controls) and immunofluorescence labeling of MPR46. However, 27% of average protein level could be a result from 1) 27% of cells expressing normal amount of protein, or 2) all cells expressing only 27% of protein, or any combination of these two. In addition, immunofluorescence does not detect labeling if the local concentration of the protein is low, such as the concentration of MPR46 on the plasma membrane. In LAMP-2–deficient hepatocytes with detectable MPR46, the receptor was found more distributed throughout the cytoplasm and less concentrated in the perinuclear region (Figure 7E).

To investigate localization of MPR46 in the TGN, we performed double immunogold labeling of MPR46 with γ-adaptin. In control hepatocytes the most concentrated MPR46 labeling was found in the Golgi region, identified by γ-adaptin labeling and the presence of a Golgi stack (Figure 8A). In LAMP-2–deficient hepatocytes the proportion of MPR46 label found in the Golgi region was reduced to 27% of the control (Table 2). With γ-adaptin double labeling it was not possible to unequivocally identify the compartments where the rest of MPR46 was located. We thus also performed double labeling of MPR46 with LAMP-1. In control hepatocytes MPR46 was frequently found in small membrane structures surrounding LAMP-1–positive multivesicular endosomes (Figure 8B). In LAMP-2–deficient hepatocytes less MPR46 labeling was observed in these structures (Figure 8C). The ratio of MPR46 labeling inside versus outside of multivesicular endosomes was 4.8 times higher in LAMP-2–deficient cells (Table 2). In addition more MPR46 was found inside autophagic vacuoles in LAMP-2–deficient cells (Figure 8, C and D). Quantitation showed that 3.9–5.2 times more MPR46 labeling was found in autophagic vacuoles (Table 2). Typically the MPR46-positive autophagic vacuoles were fusion profiles of an Avd and a multivesicular endosome (Figure 8, C and D). Taken together, our results show that in LAMP-2–deficient hepatocytes MPR46 accumulates in Avd/endosomes, suggesting that defective sorting out of endosomes leads to faster degradation of the protein.

## DISCUSSION

We have shown that intracellular retention of cathepsin-D, β-glucuronidase, and β-mannosidase is impaired in LAMP-2–deficient hepatocytes. We also could show altered localization of MPR46, including accumulation in Avd, less MPR46 in the Golgi region, and altered localization within endosomes. In control hepatocytes MPR46 was frequently found in small membrane structures surrounding LAMP-1–positive multivesicular endosomes (Figure 8B). These structures have been called "endosome associated vesicles and tubules," and they are thought to participate in MPR46

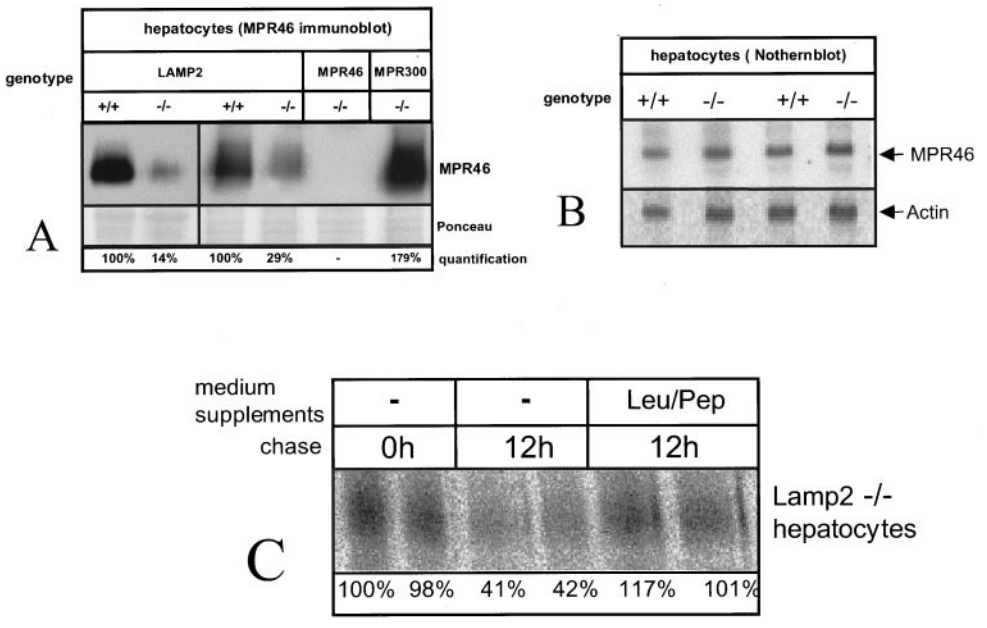


**Figure 7.** MPR46 has a shorted half-life and altered subcellular localization in LAMP-2–deficient hepatocytes. (A) Western blotting of MPR46 from control (+/+) and LAMP-2 −/− cells. MPR46−/− and MPR300 −/− hepatocytes are shown as controls. (B) Northern blotting of MPR46 and actin. (C) Immunoprecipitation of MPR46. The cells were labeled with [$^{35}$S]methionine for 12 h. Leupeptin (100 $\mu$M) and pepstatin (100 $\mu$M) were added to the chase medium as indicated (Leu/Pep). Quantitation of the bands is shown at the bottom. (D and E) Immunofluorescence of MPR46 from control (D) and LAMP-2–deficient cells (E).

recycling out of the endosomes (Klumperman *et al.*, 1993; Nicoziani *et al.*, 2000). We observed less MPR46 in these structures in LAMP-2–deficient cells (Figure 8, C and D, and Table 2). During targeting of lysosomal enzymes, MPR46 and MPR300 deliver newly synthesized enzymes to early or late endosomes (Ludwig *et al.*, 1991; Diesner *et al.*, 1993), after which they may recycle back to TGN from late endosomes. Because in LAMP-2–deficient hepatocytes, endosomes and late autophagic vacuoles readily fuse (Figure 3), both compartments can be assumed to act as starting point for receptor recycling. The ratio of MPR46 in the Golgi region versus MPR46 in endo/lysosomes and AVd was 1.81 in control and 0.28 in LAMP-2 knockout cells (Table 2). Together with the lower amount of MPR46 in endosome-associated vesicles and tubules, this suggests that the recycling of MPR46 from endosomes back to the TGN is less efficient in LAMP-2–deficient cells. However, we also observed that the transport of lipids from endo/lysosomes to the Golgi is not affected by LAMP-2 deficiency (Figure 4), suggesting that the recycling defect may be specific to MPR46.

The recycling defect may be due to a failure to sort MPR46 in endosomes. Localization to different endosomal subcompartments is known to be the basis of sorting between the endosome-to-plasma membrane recycling and early endosome-to-late endosome transport routes (Robinson *et al.*, 1996; Lemmon and Traub, 2000). MPRs are thought to recycle to the TGN from late endosomes (Hirst *et al.*, 1998; Rohn *et al.*, 2000), which are also called multivesicular bodies or the prelysosomal compartment (Griffiths *et al.*, 1988). Reduced ability to recycle MPR46 from late endosomes has been shown to lead to transport of the receptors to lysosomes where they are degraded (Schweizer *et al.*, 1996, 1997). Because the endocytic and autophagic pathways merge, we observed enrichment of MPR46 in autophagic vacuoles (Table 2). Impaired trafficking of MPR46 could

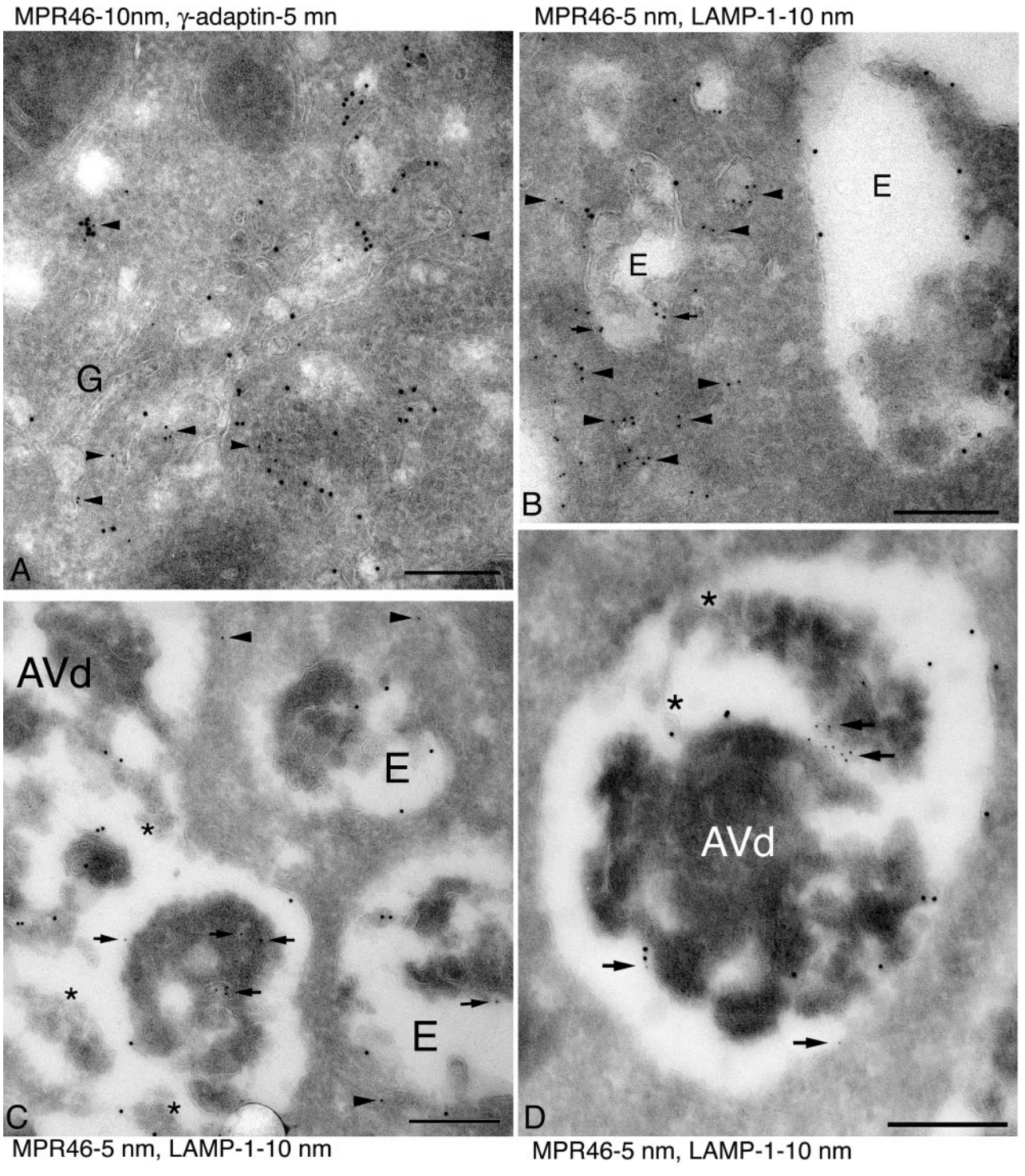


**Figure 8.** Immunogold electron microscopy of MPR46. (A) Double immunogold labeling of MPR46 (10 nm gold) and γ-adaptin (5 nm gold, arrowheads) in control cells. The most concentrated labeling is found in the Golgi region. G indicates the Golgi stack. (B–D) Double immunogold labeling of LAMP-1 (10 nm gold) and MPR46 (5 nm gold) in control (B) and LAMP-2 −/− cells (C and D). (B) In control cells MPR46 was typically located in membrane structures (arrowheads) around the endosomal vacuoles (indicated by E), and only some labeling was seen inside the endosome (arrows). (C and D) In LAMP-2 −/− cells the amount of MPR46 in membrane structures around endosomes was smaller (arrowheads), whereas more MPR46 was found inside endosomes (E) or autophagic vacuoles (AVd) (arrows). Note that in C and D the autophagic vacuoles appear to have fused with multivesicular endosomes; stars indicate some of the internal vesicles. Bars, 200 nm.

**Table 2.** Localization of MPR46 immunogold labelling (% of total) in the Golgi region and endo/lysosomal compartments in control and LAMP-2 −/− hepatocytes

| | Control | LAMP-2 −/− |
|---|---|---|
| MPR46 and γ-adaptin double labeling | | |
| Golgi region[a] | 28.0 ± 0.3 | 7.6 ± 1.3 |
| Total gold scored | 1804 | 1780 |
| MPR46 and LAMP-1 double labeling | | |
| LAMP-1–negative AVs[b] | 0.5 ± 0.1 | 2.6 ± 0.1 |
| LAMP-1–positive AVs[b] | 3.5 ± 1.6 | 13.7 ± 2.2 |
| LAMP-1–positive endo/lysosomes | 12.0 ± 2.5 | 13.0 ± 3.1 |
| Plasma membrane | 10.44 ± 1.62 | 11.73 ± 1.33 |
| Total gold scored | 2630 | 2176 |
| MPR46 inside/outside of MVB[c] | 0.17 ± 0.05 | 0.81 ± 0.2 |
| Total number of MVB scored | 43 | 46 |

The results are means ± SEM from two independent cultures of control and LAMP-2 −/− hepatocytes.

[a] Golgi region was defined by γ-adaptin labeling and presence of the Golgi stack.

[b] Autophagic vacuoles (AVs) were identified by the presence of cytoplasmic material (rough ER, mitochondria) inside the vacuoles.

[c] The ratio of labeling inside versus outside of LAMP-1–positive multivesicular endosome profiles (MVB) was estimated as described in MATERIALS AND METHODS.

explain partial mistargeting of a subset of lysosomal enzymes to the extracellular medium, which in turn could be one cause for the impaired capacity for lysosomal degradation of long-lived proteins observed in LAMP-2–deficient hepatocytes (Tanaka *et al.*, 2000). Thus, rather than by decreased fusion of autophagic vacuoles with lysosomes, the increased half-life and accumulation of autophagic vacuoles can be explained by defective lysosomal biogenesis.

In this study we observed impairment of intracellular retention for cathepsin D, β-mannosidase, and β-glucuronidase. Intracellular activity of β-hexosaminidase appeared to be increased but the proportion of activity recovered in the culture medium was comparable to controls (Table 1). This suggests that the increased intracellular activity is likely due to increased synthesis. Partial mistargeting of a subset of lysosomal enzymes is in agreement with the findings that we observed a shorter half-life of MPR46, whereas the half-life of MPR300 was comparable to controls. Both MPRs are necessary for normal targeting of lysosomal enzymes (Kasper *et al.*, 1996; Munier-Lehmann *et al.*, 1996). In addition, other lysosomal enzyme targeting mechanisms exist besides the mannose 6-phosphate mediated route (Rijnboutt *et al.*, 1991; Glickman and Kornfeld, 1993).

We observed a lower steady state level and shorted half-life for MPR46 in LAMP-2–deficient cells, whereas those of MPR300 were comparable to the control. Although the endosomal sorting and/or trafficking of both receptors may be impaired in LAMP-2–deficient cells, their susceptibility to lysosomal degradation or acidic pH may vary. Alternatively LAMP-2 deficiency may impair, directly or indirectly, recycling of MPR46 but not MPR300. In spite of being impaired in degrading autophagocytosed cytoplasm, LAMP-2–deficient hepatocytes are able to acidify autophagic vacuoles (Tanaka *et al.*, 2000).

MPR46 dissociates from its ligands in acidic environment (Hoflack and Kornfeld, 1985; Holzman, 1989; Ma *et al.*, 1991). Using the pH indicator drug DAMP, we estimated the pH of Avd to be 5.7 in control and 5.8 in LAMP-2–deficient hepatocytes (Tanaka *et al.*, 2000). Also the pH in multivesicular endosomes was close to the controls (pH 5.8) in LAMP-2–deficient hepatocytes (pH 5.9, unpublished observations). This suggests that impaired acidification in endosomes or Avd is not the cause of impaired MPR46 recycling and accumulation in Avd.

How could LAMP-2 deficiency lead to impaired recycling of MPR46 from late endosomes to the TGN? One possibility is that LAMP-2 is necessary for sorting of MPR46 inside endosomes, either directly or indirectly by stabilizing factors needed for recycling. LAMP-2 has been shown to mediate transport of a specific set of cytosolic proteins across the lysosomal membrane in chaperone-mediated autophagy (Cuervo and Dice, 1996, 1998). Thus it is possible that LAMP-2 could participate in chaperone-mediated transport of recycling promoting factors from the cytoplasm to the endosomal lumen. Another possibility is that LAMP-2 is needed to prevent transport of MPR46 from endosomes to lysosomes and thus to increase the probability that the receptor will have time to reach the endosomal subcompartment that is destined for recycling to the TGN. LAMP-2 has been shown to recycle between the lysosomal limiting membrane and matrix and thus regulate the rate of chaperone-mediated autophagy (Jadot *et al.*, 1996; Cuervo and Dice, 2000). Downregulation of chaperone-mediated autophagy by LAMP-2 levels has been proposed to mediate epidermal growth factor–induced cell growth in renal tubular cells (Franch *et al.*, 2001). These findings show that LAMP-2 is not merely a structural component of the lysosomal membrane but has more sophisticated functions.

Yet another possible explanation for the decreased intracellular protein degradation in LAMP-2–deficient cells is that LAMP-2 deficiency leads to selective disturbances in lysosomal functions, including the observed β-mannosidase deficiency, and β-glucuronidase and cathepsin-D mistargeting. LAMP-2 has been suggested to play a role in intralysosomal matrix formation (Jadot *et al.*, 1997). This could in turn lead to secondary effects such as impaired receptor recycling. It is also possible that altered trafficking of lysosomal enzymes and loss of MPR46 are separate events caused by loss of LAMP-2. Still another, although less likely explanation of altered lysosomal enzyme trafficking would be altered activity and/or localization of uncovering enzyme. This enzyme performs the final cleavage step in the biogenesis of mannose 6-phosphate tag (Faulhaber *et al.*, 1998; Rohrer and Kornfeld, 2001). Further studies are needed to differentiate between these possible connections between LAMP-2 deficiency and lysosomal enzyme targeting.

MPR46 knockout mice had a normal phenotype, although partial missorting of many lysosomal enzymes into secretion was observed in cells isolated from these mice (Köster *et al.*, 1993; Ludwig *et al.*, 1993). Lysosomal storage was not detected in liver by electron microscopy (Köster *et al.*, 1993). However, in intact tissues the increased secretion of lysosomal enzymes was shown to be compensated by uptake via

carbohydrate-specific endocytic receptors (Köster *et al.*, 1994). Our preliminary results suggest that, although fluid-phase endocytic uptake is normal, receptor-mediated endocytic uptake is impaired in LAMP-2–deficient hepatocytes, suggesting that the compensatory uptake is not functional in LAMP-2–deficient mice. This could explain the more severe phenotype in LAMP-2–deficient mice and isolated hepatocytes.

Inhibition of the phosphoinositide 3 kinase Vps34 by a dominant negative form of this enzyme has been reported to cause a similar mistargeting of cathepsin D (Row *et al.*, 2001) as observed in LAMP-2–deficient hepatocytes. On the other hand Vps34 has also been shown to be necessary for autophagosome formation (Blommaart *et al.*, 1997; Petiot *et al.*, 2000). Because we see a profound accumulation of autophagic vacuoles in LAMP-2–deficient hepatocytes, we can relatively safely conclude that Vps34 is functional in these cells and thus rule out Vps34 deficiency as an explanation of the defect in lysosomal enzyme targeting.

Why do we only see accumulation of autophagic vacuoles in some tissues of LAMP-2–deficient mice, including pancreas, liver parenchyme, heart, muscle, capillary endothelium of kidney, intestinal wall, lymph nodes, and neutrophilic leukocytes (Tanaka *et al.*, 2000), while other tissues such as brain and fibroblasts seem to be normal? Many of the affected tissues in LAMP-2–deficient mice are those that have a high degree of autophagy in normal animals. Using mainly rat tissues, active autophagy has been described at least in liver (Pfeifer and Strauss, 1981; Kovacs *et al.*, 1982; de Waal *et al.*, 1986), pancreas (Kovacs *et al.*, 1988), muscle (Salminen and Vihko, 1984; Bahro *et al.*, 1992), heart (Pfeifer and Strauss, 1981; Dammrich and Pfeifer, 1983), and kidney (Pfeifer and Scheller, 1975; Bahro *et al.*, 1988). This suggests that active ongoing autophagy in normal conditions may be the prerequisite for the observed phenotype of autophagic vacuole accumulation in LAMP-2–deficient tissues.

It should be noted that the structurally related LAMP-1 might compensate in part for the loss of LAMP-2 in LAMP-2–deficient mice. These compensating functions are supported by the phenotype of LAMP-1/LAMP-2 double-deficient mice. Although the single-deficient mice are fertile and viable (Andrejewski *et al.*, 1999; Tanaka *et al.*, 2000), the loss of both LAMP molecules leads to embryonic lethality associated with accumulation of autophagic vacuoles in almost all embryonic tissues (P. Saftig, unpublished data).

In summary, instead of being only a structural component of the lysosomal membrane, LAMP-2 plays a more dynamic role than previously anticipated in cellular processes such as macro autophagy, chaperone-mediated autophagy, and receptor trafficking. To further elucidate the postulated LAMP-2 function in receptor sorting and/or trafficking, it will be important to identify possible binding partners of LAMP-2. Coimmunoprecipitation and yeast two-hybrid screen experiments will possibly bring more light to this intriguing question.

## ACKNOWLEDGMENTS

We are grateful to Ellen Eckerman and Anegret Schneeman for technical assistance. This study was funded by a grant from the Deutsche Forschungsgemeinschaft (SA683/1–3) and the Fonds der Chemischen Industrie to P.S., a grant from The Royal Society to E.-L.E, and grants from the Ministry of Labor, Health, and Welfare of Japan and the Ministry of Education, Science, Sports, and Culture of Japan to Y.T. A.L.I. was supported by the Graduiertenkolleg 60.

## REFERENCES

Andrejewski, N., Punnonen, E.L., Guhde, G., Tanaka, Y., Lullmann-Rauch, R., Hartmann, D., von Figura, K., and Saftig, P. (1999). Normal lysosomal morphology and function in LAMP-1-deficient mice. J. Biol. Chem. *274*, 12692–12701.

Arstila, A.U., and Trump, B.F. (1968). Studies on cellular autophagocytosis. The formation of autophagic vacuoles in the liver after glucagon administration. Am. J. Pathol. *53*, 687–733.

Bahro, M., Gertig, G., and Pfeifer, U. (1988). Short-term stimulation of cellular autophagy by furosemide in the thick ascending limb of Henle's loop in the rat kidney. Cell Tissue Res. *253*, 625–629.

Bahro, M., Pfeifer, U., and Dammrich, J. (1992). Involvement of autophagic degradation in ACTH-induced skeletal muscle atrophy. Clin. Neuropathol. *11*, 64–70.

Blommaart, E.F.C., Krause, U., Schellens, J.P.M., Vreeling-Sindelarova, H., and Meijer, A.J. (1997). The phosphatidyl-inositol 3-kinase inhibitors wortmannin and LY294002 inhibit autophagy in isolated rat hepatocytes. Eur. J. Biochem. *243*, 240–246.

Claussen, M., Buergisser, D., Schuller, A.G., Matzner, U., and Braulke, T. (1995). Regulation of insulin-like growth factor (IGF)-binding protein-6 and mannose 6-phosphate/IGF-II receptor expression in IGF-IL-overexpressing NIH 3T3 cells. Mol. Endocrinol. *9*, 902–912.

Cuervo, A.M., and Dice, J.F. (1996). A receptor for the selective uptake and degradation of proteins by lysosomes. Science *273*, 501–503.

Cuervo, A.M., and Dice, J.F. (1998). Lysosomes, a meeting point of proteins, chaperones, and proteases. J. Mol. Med. *76*, 6–12.

Cuervo, A.M., and Dice, J.F. (2000). Regulation of Lamp2a Levels in the Lysosomal Membrane. Traffic *1*, 570–583.

Dammrich, J., and Pfeifer, U. (1983). Cardiac hypertrophy in rats after supravalvular aortic constriction. II. Inhibition of cellular autophagy in hypertrophying cardiomyocytes. Virchows Arch. B Cell Pathol. Incl. Mol. Pathol. *43*, 287–307.

de Waal, E.J., Vreeling-Sindelarova, H., Schellens, J.P.M., Houtkooper, J.M., and James, J. (1986). Quantitative changes in the lysosomal vacuolar system of rat hepatocytes during short-term starvation. A morphometric analysis with special reference to macro- and microautophagy. Cell Tissue Res. *243*, 641–648.

Diesner, F., Sommerlade, H.J., and Braulke, T. (1993). Transport of newly synthesized arylsulfatase A to the lysosome via transferrin receptor-positive compartments. Biochem. Biophys. Res. Commun. *197*, 1–7.

Dunn, W.A. (1994). Autophagy and related mechanisms of lysosomal-mediated protein degradation. Trends Cell Biol. *4*, 139–143.

Fambrough, D.M., Takeyasu, K., Lippincott-Schwarz, J., and Siegel, N.R. (1988). Structure of LEP100, a glycoprotein that shuttles between lysosomes and the plasma membrane, deduced from the nucleotide sequence of the encoding cDNA. J. Cell Biol. *106*, 61–67.

Faulhaber, J., Fensom, A., and Hasilik, A. (1998). Abnormal lysosomal sorting with an enhanced secretion of cathepsin D precursor molecules bearing monoester phosphate groups. Eur J. Cell Biol. *77*, 134–140.

Febbraio, M., and Silverstein, R.L. (1990). Identification and characterization of Lamp-1 as an activation-dependent platelet surface glycoprotein. J. Biol. Chem. *265*, 18531–18537.

Franch, H.A., Sooparb, S., and Du, J. (2001). A mechanism regulating proteolysis of specific proteins during renal tubular cell growth. J. Biol. Chem. *276*, 19126–19131.

Fukuda, M. (1991). Lysosomal membrane glycoproteins. Structure, biosynthesis, and intracellular trafficking. J. Biol. Chem. *266*, 21327–21330.

Glickman, J.N., and Kornfeld, S. (1993). Mannose 6-phosphate-independent targeting of lysosomal enzymes in I-cell disease B lymphoblasts. J. Cell Biol. *123*, 99–108.

Granger, B.L., Green, S.A., Gabel, C.A., Howe, C.L., Mellman, I., and Helenius, A. (1990). Characterization and cloning of lgp110, a lysosomal membrane glycoprotein from mouse and rat cells. J. Biol. Chem. *265*, 12036–12043.

Griffiths, G., Hoflack, B., Simons, K., Mellman, I., and Kornfeld, S. (1988). The mannose 6-phosphate receptor and the biogenesis of lysosomes. Cell *52*, 329–3241.

Guarnieri, F.G., Arterburn, L.M., Penno, M.B., Cha, Y., and August, J.T. (1993). The motif Tyr-X-X-hydrophobic residue mediates lysosomal membrane targeting of lysosome-associated membrane protein 1. J. Biol. Chem. *268*, 1941–1946.

Hille-Rehfeld, A. (1995). Mannose 6-phosphate receptors in sorting and transport of lysosomal enzymes. Biochem Biophys Acta. *1241*, 177–194.

Hirst, J., Futter, C.E., and Hopkins, C.R. (1998). The kinetics of mannose 6-phosphate receptor trafficking in the endocytic pathway in HEp-2 cells: the receptor enters and rapidly leaves multivesicular endosomes without accumulating in a prelysosomal compartment. Mol. Biol. Cell *9*, 809–816.

Hoflack, B., and Kornfeld, S. (1985). Purification and characterization of a cation-dependent mannose 6-phosphate receptor from murine P388D1 macrophages and bovine liver. J. Biol. Chem. *260*, 12008–12014.

Holzman, E. (1989). Lysosomes. New York: Plenum Press, 439 pp.

Höning, S., and Hunziker, W. (1995). Cytoplasmic determinants involved in direct lysosomal sorting, endocytosis, and basolateral targeting of rat lgp120 (lamp-1) in MDCk cells. J. Cell Biol. *128*, 464–473.

Howard, C.V., and Reed, M.G. (1998). Unbiased stereology. Three-dimensional measurement in microscopy. New York: Springer-Verlag, 246 pp.

Isbrandt, D., Arlt, G., Brooks, D.A., Hopwood, J.J., von Figura, K., and Peters, C. (1994). Mucopolysaccharidosis VI (Maroteaux-Lamy syndrome): six unique arylsulfatase B gene alleles causing variable disease phenotypes. Am. J. Hum. Genet. *54*, 454–463.

Jadot, M., Dubois, F., Wattiaux-De Coninck, S., and Wattiaux, R. (1997). Supramolecular assemblies from lysosomal matrix proteins and complex lipids. Eur. J. Biochem. *249*, 862–869.

Jadot, M., Wattiaux, R., Mainferme, F., Dubois, F., Claessens, A., and Wattiaux-De Coninck, S. (1996). Soluble form of Lamp II in purified rat liver lysosomes. Biochem. Biophys. Res. Commun. *223*, 353–359.

Kasper, D., Dittmer, F., von Figura, K., and Pohlmann, R. (1996). Neither type of mannose 6-phosphate receptor is sufficient for targeting of lysosomal enzymes along intracellular routes. J. Cell Biol. *134*, 615–623.

Klionsky, D.J., and Emr, S.D. (2000). Autophagy as a regulated pathway of cellular degradation. Science *290*, 1717–1721.

Klumperman, J., Hille, A., Veenendaal, T., Oorschot, V., Stoorvogel, W., von Figura, K., and Geuze, H.J. (1993). Differences in the endosomal distributions of the two mannose 6-phosphate receptors. J. Cell Biol. *121*, 997–1010.

Kornfeld, S., and I. Mellman. (1989). The biogenesis of lysosomes. Annu Rev Cell Biol. *5*, 483–525.

Köster, A., Nagel, G., von Figura, K., and Pohlmann, R. (1991). Molecular cloning of the mouse 46-kDa mannose 6-phosphate receptor (MPR 46). Biol. Chem. Hoppe Seyler *372*, 297–300.

Köster, A., Saftig, P., Matzner, U., von Figura, K., Peters, C., and Pohlmann, R. (1993). Targeted disruption of the Mr 46 000 mannose 6-phosphate receptor gene in mice results in misrouting of lysosomal proteins. EMBO J. *12*, 5219–5223.

Köster, A., von Figura, K., and Pohlmann, R. (1994). Mistargeting of lysosomal enzymes in Mr46 000 mannose 6-phosphate receptor-deficient mice is compensated by carbohydrate-specific endocytotic receptors. Eur. J. Biochem. *224*, 685–689.

Kovacs, A.L., Reith, A., and Seglen, P.O. (1982). Accumulation of autophagosomes after inhibition of hepatocytic protein degradation by vinblastine, leupeptin or a lysosomotropic amine. Exp. Cell Res. *137*, 191–201.

Kovacs, J., Laszlo, L., and Kovacs, A.L. (1988). Regression of autophagic vacuoles in pancreatic acinar, seminal vesicle epithelial, and liver parenchymal cells: a comparative morphometric study of the effect of vinblastine and leupeptin followed by cycloheximide treatment. Exp. Cell Res. *174*, 244–251.

Lee, N., Wang, W.C., and Fukuda, M. (1990). Granulocytic differentiation of HL-60 cells is associated with increase of poly-*N*-acetyllactosamine in Asn-linked oligosaccharides attached to human lysosomal membrane glycoproteins. J. Biol. Chem. *265*, 20476–20487.

Lehmann, L.E., Eberle, W., Krull, S., Prill, V., Schmidt, B., Sander, C., von Figura, K., and Peters, C. (1992). The internalization signal in the cytoplasmic tail of lysosomal acid phosphatase consists of the hexapeptide PGYRHV. EMBO J. *11*, 4391–4399.

Lemmon, S.K., and Traub, L.M. (2000). Sorting in the endosomal system in yeast and animal cells. Curr. Opin. Cell Biol. *12*, 457–466.

Lewis, V., Green, S.A., Marsh, M., Vihko, P., Helenius, A., and Mellman, I. (1985). Glycoproteins of the lysosomal membrane. J. Cell Biol. *100*, 1839–1847.

Lippincott-Schwartz, J., and Fambrough, D.M. (1987). Cycling of the integral membrane glycoprotein, LEP100, between plasma membrane and lysosomes: kinetic and morphological analysis. Cell *49*, 669–677.

Lloyd, J.B., and Forster, S. (1986) The lysosome membrane. TIBS. *11*, 365–368.

Ludwig, T., Griffiths, G., and Hoflack, B. (1991). Distribution of newly synthesized lysosomal enzymes in the endocytic pathway of normal rat kidney cells. J. Cell Biol. *115*, 1561–1572.

Ludwig, T., Ovitt, C.E., Bauer, U., Hollinshead, M., Remmler, J., Lobel, P., Ruther, U., and Hoflack, B. (1993). Targeted disruption of the mouse cation-dependent mannose 6-phosphate receptor results in partial missorting of multiple lysosomal enzymes. EMBO J. *12*, 5225–5235.

Ma, Z.M., Grubb, J.H., and Sly, W.S. (1991). Cloning, sequencing, and functional characterization of the murine 46-kDa mannose 6-phosphate receptor. J. Biol. Chem. *266*, 10589–10595.

Meredith, M.J. (1988). Rat hepatocytes prepared without collagenase: prolonged retention of differentiated characteristics in culture. Cell Biol. Toxicol. *4*, 405–425.

Mitchener, J.S., Shelburne, J.D., Bradford, W.D., and Hawkins, H.K. (1976). Cellular autophagocytosis induced by deprivation of serum and amino acids in HeLa cells. Am. J. Pathol. *83*, 485–491.

Mortimore, G.E., Poso, A.R., and Lardeux, B.R. (1989). Mechanism and regulation of protein degradation in liver. Diabetes Metab. Rev. *5*, 49–70.

Munier-Lehmann, H., Mauxion, F., Bauer, U., Lobel, P., and Hoflack, B. (1996). Re-expression of the mannose 6-phosphate receptors in receptor-deficient fibroblasts. Complementary function of the two mannose 6-phosphate receptors in lysosomal enzyme targeting. J. Biol. Chem. *271*, 15166–15174.

Nicoziani, P., Vilhardt, F., Llorente, A., Hilout, L., Courtoy, P.J., Sandvig, K., and van Deurs, B. (2000). Role for dynamin in late endosome dynamics and trafficking of the cation-independent mannose 6-phosphate receptor. Mol. Biol. Cell *11*, 481–495.

Nishino, I. *et al.* (2000). Primary LAMP-2 deficiency causes X-linked vacuolar cardiomyopathy and myopathy (Danon disease). Nature *406*, 906–910.

Peters, C., and von Figura, K. (1994). Biogenesis of lysosomal membranes. FEBS Lett. *346*, 146–150.

Petiot, A., Ogier-Denis, E., Blommaart, E.F.C., Meijer, A.J., and Codogno, P. (2000). Distinct classes of phosphatidyl-inositol 3′-kinase are involved in signaling pathways that control macroautophagy in HT-29 cells. J. Biol. Chem. *275*, 992–998.

Pfeifer, U., and Scheller, H. (1975). A morphometric study of cellular autophagy including diurnal variations in kidney tubules of normal rats. J. Cell Biol. *64*, 608–621.

Pfeifer, U., and Strauss, P. (1981). Autophagic vacuoles in heart muscle and liver. A comparative morphometric study including circadian variations in meal-fed rats. J. Mol. Cell. Cardiol. *13*, 37–49.

Pohlmann, R., Wendland, M., Boeker, C., and von Figura, K. (1995). The two mannose 6-phosphate receptors transport distinct complements of lysosomal proteins. J. Biol. Chem. *270*, 27311–27318.

Rijnboutt, S., Kal, A.J., Geuze, H.J., Aerts, H., and Strous, G.J. (1991). Mannose 6-phosphate-independent targeting of cathepsin D to lysosomes in HepG2 cells. J. Biol. Chem. *266*, 23586–23592.

Robinson, M.S., Watts, C., and Zerial, M. (1996). Membrane dynamics in endocytosis. Cell *84*, 13–21.

Rohn, W.M., Rouille, Y., Waqguri, S., and Hoflack, B. (2000). Bidirectional trafficking between the trans-Golgi network and the endosomal/lysosomal system. J. Cell Sci. *113*, 2093–2101.

Rohrer, J., and Kornfeld, S. (2001). Lysosomal hydrolase mannose 6-phosphate uncovering enzyme resides in the trans-Golgi network. Mol. Biol. Cell *12*, 1623–1631.

Row, P.E., Reaves, B.J., Domin, J., Luzio, J.P., and Davidson, H.W. (2001). Overexpression of a rat kinase-deficient phosphoinositide 3-kinase, Vps34p, inhibits cathepsin D maturation. Biochem. J. *353*, 655–661.

Salminen, A., and Vihko, V. (1984). Autohagic response to strenuous exercise in mouse skeletal muscle fibers. Virchovs Arch. B Cell Pathol. Incl. Mol. Pathol. *45*, 97–106.

Schwarzmann, G. (2001). Uptake and metabolism of exogenous glycosphingolipids by cultured cells. Sem. Cell. Dev. Biol. *12*, 163–171.

Schwarzmann, G., Hofmann, P., Putz, U., and Albrecht, B. (1995). Demonstration of direct glycosylation of nondegradable glycosylceramide alalogs in cultured cells. J. Biol. Chem. *270*, 21271–21276.

Schwarzmann, G., and Sandhoff, K. (1990). Metabolism and intracellular transport of glycosphingolipids. Biochemistry *29*, 10865–10871.

Schweizer, A., Kornfeld, S., and Rohrer, J. (1996). Cysteine34 of the cytoplasmic tail of the cation-dependent mannose 6-phosphate receptor is reversibly palmitoylated and required for normal trafficking and lysosomal enzyme sorting. J. Cell Biol. *132*, 577–584.

Schweizer, A., Kornfeld, S., and Rohrer, J. (1997). Proper sorting of the cation-dependent mannose 6-phosphate receptor in endosomes depends on a pair of aromatic amino acids in its cytoplasmic tail. Proc. Natl. Acad. Sci. USA *94*, 14471–14476.

Seglen, P.O. (1987). Regulation of autophagic protein degradation in isolated liver cells. In: Lysosomes: Their Role in Protein Breakdown, ed. H. Glaumann and F.J. Ballard, London: Orlando, 371–414.

Seglen, P.O., and Bohley, P. (1992). Autophagy and other vacuolar protein degradation mechanisms. Experientia *48*, 158–172.

Seglen, P.O., and Gordon, P.B. (1982). 3-methyladenine: specific inhibitor of autophagic/lysosomal protein degradation in isolated rat hepatocytes. Proc. Natl. Acad. Sci. USA *79*, 1889–1892.

Seglen, P.O., and Gordon, P.B. (1984). Amino acid control of autophagic sequestration and protein degradation in isolated hepatocytes. J. Cell Biol. *99*, 435–444.

Slot, J.W., and Geuze, H.J. (1985). A new method of preparing gold probes for multiple-labeling cytochemistry. Eur J. Cell Biol. *38*, 87–93.

Talloczy, Z., W. Jiang, H.W. Virgin IV, D. Leib, D. Scheuner, R. Kaufman, E.L. Eskelinen, and B. Levine. (2002). Regulation of starvation and virus-induced autophagy by the eIF2alpha kinase signaling pathway. Proc. Natl. Acad. Sci. USA *99*, 190–195.

Tanaka, Y. *et al.* (2000). Accumulation of autophagic vacuoles and cardiomyopathy in LAMP-2-deficient mice. Nature *406*, 902–906.

Waheed, A., Gottschalk, S., Hille, A., Kreutler, C., Pohlmann, R., Braulke, T., Hauser, H., Geuze, H., and von Figura, K. (1988). Human lysosomal acid phosphatase is transported as a transmembrane protein to lysosomes in transfected baby hamster kidney cells. EMBO J. *7*, 2351–2358.

Wenk, J., Hille, A., and von Figura, K. (1991). Quantitation of Mr 46000 and Mr 300000 mannose 6-phosphate receptors in human cells and tissues. Biochem. Int. *23*, 723–731.

Williams, M.A., and McCluer, R.H. (1980). The use of Sep-Pak C18 cartridges during the isolation of gangliosides. J Neurochem. *35*, 266–269.

Yamamoto, K., Katsuda, N., Himeno, M., and Kato, K. (1979). Cathepsin D of rat spleen: affinity purification and properties of two types of cathepsin D. Eur. J. Biochem. *95*, 459–467.